The American Journal of Pathology, Vol. 173, No. 5, November 2008

DOI: 10.2353/ajpath.2008.080098

Molecular Pathogenesis of Genetic and Inherited Diseases

Dysferlin Deficiency Shows Compensatory Induction of Rab27A/Slp2a That May Contribute to Inflammatory Onset

Akanchha Kesari,* Mitsunori Fukuda,† Susan Knoblach,* Rumaisa Bashir,‡ Gustavo A. Nader,* Deepak Rao,* Kanneboyina Nagaraju,* and Eric P. Hoffman*

From the Research Center for Genetic Medicine, Children's National Medical Center, Washington DC; Department of Developmental Biology and Neurosciences,† Tohoku University, Miyagi, Japan; and School of Biological and Biochemical Sciences,‡ University of Durham, Durham, United Kingdom*

Mutations in the dysferlin gene cause limb girdle muscular dystrophy 2B (LGMD2B) and Miyoshi myopathy. Dysferlin-deficient cells show abnormalities in vesicular traffic and membrane repair although onset of symptoms is not commonly seen until the late teenage years and is often associated with subacute onset and marked muscle inflammation. To identify molecular networks specific to dysferlin-deficient muscle that might explain disease pathogenesis, muscle mRNA profiles from 10 mutation-positive LGMD2B/MM patients were compared with a disease control [LGMD2I; (n = 9)], and normal muscle samples (n = 11). Query of inflammatory pathways suggested LGMD2B-specific increases in co-stimulatory signaling between dendritic cells and T cells (CD86, CD28, and CTLA4), associated with localized expression of both versican and tenascin. LGMD2B muscle also showed an increase in vesicular trafficking pathway proteins not normally observed in muscle (synaptotagmin-like protein Slp2a/SYTL2 and the small GTPase Rab27A). We propose that Rab27A/Slp2a expression in LGMD2B muscle provides a compensatory vesicular trafficking pathway that is able to repair membrane damage in the absence of dysferlin. However, this same pathway may release endocytotic vesicle contents, resulting in an inflammatory microenvironment. As dysferlin deficiency has been shown to enhance phagocytosis by macrophages, together with our findings of abnormal myofiber endocytosis pathways and dendritic-T cell activation markers, these results suggest a model of immune and inflammatory network over-stimulation that may explain the subacute inflammatory presentation. ***(Am J Pathol 2008, 173:1476–1487; DOI: 10.2353/ajpath.2008.080098)***

Limb-girdle muscular dystrophies are a group of heterogeneous disorders typically showing an autosomal recessive mode of inheritance, progressive muscle weakness, and high serum creatine kinase levels.[1] Two types of muscle disease, a distal myopathy (Miyoshi Myopathy, MM) and a form of limb girdle muscular dystrophy (LGMD2B) have both been shown to be caused by mutations of the dysferlin gene.[2,3] In both LGMD2B and MM, dysferlin gene mutations result in partial or complete loss of dysferlin protein in muscle as measured by immunoassays, although the reduction in dysferlin levels does not strictly correlate with clinical severity.[4] Both the proximal (LGMD2B) and distal (MM) phenotypes can be caused by identical mutations in the same family, suggesting the role of genetic modifiers and/or environmental influence on disease expression.[5] The dysferlin gene is localized to 2p13 with expression in various tissues ranging from kidney to monocytes, with highest levels in skeletal and cardiac muscle.[6] Dysferlin is localized predominantly to the muscle surface membrane, and is also associated with cytoplasmic vesicles.[7]

The dysferlin protein was originally named based on its similarity to the *Caenorhabditis elegans* protein FER-1. FER-1 is responsible for mediating fusion of intracellular vesicles with the spermatid plasma membrane.[8] Sequence homology between FER-1 and dysferlin includes

Supported in part by grants from the National Institutes of Health (5R01NS029525; Intellectual and Developmental Disabilities Research Center 1P30HD40677-06; National Center for Medical Rehabilitation Research 5R24HD050846-02) (to EPH) and [RO1-AR050478 and 5U54HD053177to KN, and the Jain Foundation].

Accepted for publication July 29, 2008.

Supplemental material for this article can be found on http://ajp.amjpathol.org.

Address reprint requests to Eric P. Hoffman, Research Center for Genetic Medicine, Children's National Medical Center, 111 Michigan Ave NW, Washington DC 20010. Email: ehoffman@cnmcresearch.org.

tandem C2 domains and a C terminal transmembrane domain. The similarity in primary structure of the two proteins led to the suggestion that dysferlin may also play a role in membrane fusion events in skeletal muscle cells.[9] C2 domains are known to bind calcium, phospholipids or proteins to trigger signaling events and membrane trafficking, and this has led to speculation that dysferlin is important for membrane repair in skeletal muscle.[2,10] This hypothesis is supported by the finding that dysferlin deficient patient muscle shows numerous structural membrane defects when analyzed by electron microscopy, including tears in the plasma membrane and an accumulation of subsarcolemmal vesicles and vacuoles.[11] Also, laser-induced membrane damage in dysferlin-deficient myofibers has highlighted reduced membrane resealing capability compared to normal muscle myofibers.[12] These findings are consistent with a plasma membrane repair defect in dysferlin-deficient myofibers.

The current understanding of molecular and cellular defects in LGMD2B/MM does not explain a number of the enigmatic features of the presentation and progression of patients with dysferlin deficiency in muscle. First, dysferlin-deficient patients are typically quite healthy until their late teens, and in our patient cohort some patients showed impressive athletic skill at young age, before disease onset. Second, disease onset is typically in late teens or early twenties, and is often associated with a subacute onset of weakness, with marked muscle inflammation on muscle biopsy.[13,14] The onset and inflammation often leads to the misdiagnosis of polymyositis.[14,15] Finally, the relatively wide inter- and intrafamilial variation in clinical phenotype, subacute onset, and marked inflammation suggest that environmental factors, other genetic modifiers, or both may play a stronger role in LGMD2B than in the other dystrophies.

The aggressive inflammation often observed in dysferlin-deficient muscle distinguishes it from other Limb-girdle dystrophies. Systematic studies of the inflammatory cell content showed a predominance of macrophages, and $CD4^+$ cells, however CD8+ cytotoxic T cells are also abundant.[11,13,14] Normal monocytes contain dysferlin, and LGMD2B/MM patients lack dysferlin in their monocytes.[16,17] We have recently shown that dysferlin-deficient monocytes display abnormal signaling and phagocytotic activity that could contribute to excessive inflammation in patient muscle.[18] Further, human LGMD2B and mouse (SJL) dysferlin-deficient muscle showed macrophage and dendritic cell activation markers, including HLA-DR, HLA-ABC, and CD86 (human), and MOMA-2, CD11c, and ICAM-1 (mice) suggesting that mild myofiber damage in dysferlin-deficient muscle may result in an exaggerated monocyte/dendritic cell response secondary to dysferlin protein loss.

In the present study, we sought to identify the novel networks induced as a direct consequence of dysferlin deficiency. Key to our approach is the filtering out of molecular changes resulting from non-specific muscle pathology (degeneration, regeneration, fibrosis, and inflammation). To accomplish this, we compared a series of dysferlin-deficient, mutation-positive LGMD2B/Miyoshi patient muscle biopsy profiles to a muscular dystrophy of similar age of onset and clinical severity, LGMD2I, involving partial loss-of-function of FKRP (fukutin-related protein). We also included muscle biopsies from normal volunteers, Becker muscular dystrophy, and amyotrophic lateral sclerosis as additional controls. This approach led to the identification of both vesicle trafficking and inflammatory changes that were specific to or strongly exaggerated in dysferlin-deficient muscle.

Materials and Methods

Patients

The patient population in the study was taken from a molecular diagnostic referral population. Frozen muscle biopsies from patients with a tentative diagnosis of muscular dystrophy were sent to the Hoffman laboratory at Children's National Medical Center, Washington DC. All samples were subjected to a standardized set of biochemical and histological assays. Tests included hematoxylin and eosin histological stains, dystrophin immunostaining, α-sarcoglycan immunostaining, merosin (laminin alpha2) immunostaining, dystrophin immunoblotting and dysferlin immunoblotting, as previously described.[19] Patients were recruited and samples were analyzed under protocol 2405, which has been reviewed and approved by the Office for the Protection of Human Subjects at Children's National Medical Center.

Muscle biopsies from four groups of subjects were studied for mutation and expression profiling studies: dysferlin deficient, FKRP (LGMD2I), Becker muscular dystrophy, normal volunteers (exercise studies), and amyotrophic lateral sclerosis (ALS). For dysferlin-deficient biopsies used in this study, twenty five patient biopsies showed complete or greatly reduced dysferlin signal by duplicate immunoblots (Table 1), and these patients were then used for subsequent dysferlin DNA mutation studies, mRNA profiling, and protein characterizations. For LGMD2I subjects, approximately 1000 frozen muscle biopsies from the diagnostic muscle tissue bank were selected, genomic DNA prepared from muscle cryosections, and mutation screening for the FKRP gene was done (see Materials and Methods). For Becker muscular dystrophy, patient biopsies showed dystrophin of abnormal size and quantity by duplicate immunoblots, and showed dystrophin gene deletion mutations. For ALS, patients were diagnosed by El Escorial criteria. Normal controls were from normal volunteers enrolled in exercise studies, and different biopsies used for mRNA profiling and protein validation studies.

Genomic DNA Analysis

For dysferlin-deficient patients, twenty five patients showing complete or greatly reduced dysferlin by duplicate immunoblots were selected, and genomic DNA was isolated from 10 mg of flash-frozen muscle biopsy using Genomic DNA Purification Kit (Gentra Systems Minneapolis, MA). 10 ng of the genomic DNA was used as a template for amplification of each of the 55 exons of the dysferlin gene using

Table 1. Biochemical and Molecular Features with Mutations in Dysferlin Deficient (LGMD2B/MM) and FKRP (LGMD2I) Patients

PN	Sex	Age at biopsy (yr)	Dysferlin deficiency	Nucleotide change	Outcome of mutation	Novel mutation	Microarray
LGMD2B/Miyoshi Subjects							
D1	F	19	Complete	c.610C>T	p.Arg203X	No	Yes
				c.4192_4193insC	p.Cys1398SerfsX11	Yes	
D2	F	NA	Complete	c.3113G>A	p.Arg1038Gln	No	Yes
				c.1749_1750insT	p.Glu584X	Yes	
D3	F	31	Complete	c.2779delG	p.Ala927LeufsX21	Yes	Yes
				c.4253G>A	p.Gly1418Asp	Yes	
D4	M	27	Complete	c.3992G>T	p.Arg1331Leu	No	Yes
				c.3972C>T	ESE		
D5	F	42	Complete	c.2902A>T	p.Met968Leu	Yes	Yes
				c.3181delC	p.Gln1061ArgfsX59	Yes	
D6	F	41	Complete	c.539dupC	p.Ala181GlyfsX29	Yes	Yes
				c.1402C>T	p.Arg468Cys	Yes	
D7	M	41	Complete	c.2779delG	p.Ala927LeufsX21	Yes	Yes
				c.857T>A	p.Val286Glu	Yes	
D8	M	20	Partial	c.6124C>T	pArg2042Cys	No	Yes
				ND			
D9	F	12	Complete	c.1178_1180+dup	splice Mutation	Yes	Yes
				ND			
D10	M	16	Complete	c.1834C>T	p.Gln612X	No	Yes
				180 bp intronic deletion			
D11	M	16	Partial	c.5194G>C	p.Glu1732Gln	Yes	No
				c.3181delC	p.Gln1061ArgfsX59	Yes	No
D12	F	34	Partial	c.2997G>T	p.Trp999Cys	No	No
				ND			
D13	M	54	Partial	c.5430–2A>G	splice Mutation	Yes	No
				ND			
D14	M	43	Complete	c.4943A>G	p.Tyr1648Cys	Yes	No
				c.4943A>G	p.Tyr1648Cys	Yes	No
D15	F	18	Complete	c.3113G>A	p.Arg1038Gln	No	No
				ND			
D16	M	21	Partial	c.6124C>T	pArg2042Cys	No	No
				ND			
D17	F	26	Complete	c.2643 + 1G>A	splice Mutation	No	No
				c.4167 + 1G>C	splice Mutation	No	No
D18	M	37	Complete	c.2641A>C	p.Thr881Pro	No	No
				ND			
D19	M	22	Complete	c.5835_5838del	p.Gln1946TrpfsX18	No	No
				c.5835_5838del	p.Gln1946TrpfsX18	No	No
LGMD2I/FKRP Subjects							
F1	F	25	Normal	c.826C>A	p.Leu276Ile	No	Yes
				c.586G>C	p.Gly196Arg	No	
F2	F	16	Normal	c.826C>A	p.Leu276Ile	No	Yes
				c.826C>A	p.Leu276Ile	No	
F3	M	12	Normal	c.826C>A	p.Leu276Ile	No	Yes
				ND			
F4	M	40	Normal	c.427C>A	p.Arg143Ser	No	Yes
				ND			
F5	F	22	Normal	c.427C>A	p.Arg143Ser	No	Yes
				ND			
F6	M	10	Normal	c.427C>A	p.Arg143Ser	No	Yes
				c.427C>A	p.Arg143Ser	No	
F7	M	6	Normal	c.826C>A	p.Leu276Ile	No	Yes
				c.826C>A	p.Leu276Ile	No	
F8	F	31	Normal	c.826C>A	p.Leu276Ile	No	Yes
				c.826C>A	p.Leu276Ile	No	
F9	M	NA	Normal	c.826C>A	p.Leu276Ile	No	Yes

NA, Not available, ND, Not detected, PN, Patient Number.

dysferlin specific intronic primers. Primers were designed using the PRIMER 3 software and amplification was performed using ABI Ampli Taq Gold reagents (Foster City, CA). PCR products were screened for base changes by using denaturing high-pressure liquid chromatography on a Transgenomic Wave DNA Fragment Analysis System (San Jose, CA).[20] Melting temperature profiles were determined by sequence analysis of PCR products by using WaveMaker 4.0 software (Transgenomics, Inc., San Jose, CA). For regions containing potential heteroduplexes by denaturing high-pressure liquid chromatography, direct, automated sequencing was performed by using cycle sequencing reactions (Big Dye TM Terminator v3.1; Applied Biosystems, Foster City, CA). An ABI 3130-Genetic Analyzer (Applied Biosystems) was used for

sequencing. Data were analyzed with Sequencher TM 4.1.4 (Gene Codes Corporation, Ann Arbor, MI).

For LGMD2I patients, genomic DNA was extracted as described above from approximately 1000 muscle biopsies. Each DNA sample were first screened for the common mutation [*c.826C>A (p.Leu276Ile)*][21] using a TaqMan allele discrimination assay. Those showing heterozygosity for p.Leu276Ile were then subjected to DNA sequencing.

Mutation numbering is based on DYSF or FKRP cDNA (with sequence position 1 being the A in the first ATG codon). A "c." and "p." prefix, respectively, denotes to cDNA and protein sequences. The reference sequences used were derived from GenBank ID NM_003494.2 (Dysferlin), or GenBank ID NM_024301.2 (FKRP). Mutations were detected by sequencing both strands and were confirmed by resequencing of newly amplified PCR products. All mutations have been deposited in the Leiden Muscular Dystrophy database (Center for Human and Clinical Genetics, Leiden University Medical Center; *http://www.dmd.nl/*).

mRNA Expression Profiling

RNA was extracted from ten dysferlin deficient, nine fukutin-related protein (FKRP) mutation positive samples, eleven normal volunteers, and seven ALS muscle biopsy samples using the Trizol (Invitrogen Carsland, CA) method followed by further purification on RNeasy columns. Isolated RNA from each individual sample was used to prepare biotinylated cRNA target according to manufacture protocols (Affymetrix, CA). Twenty micrograms of biotinylated cRNAs from samples were fragmented and hybridized to 37 individual Affymetrix GeneChip HG U133 Plus2 (Affymetrix, Santa Clara, CA) for 16 hours. The arrays were washed and stained on the Affymetrix Fluidics station 400, using instructions and reagents provided by Affymetrix. This involves removal of non-hybridized material, and then incubation with phycoerythrin-streptavidin to detect bound cRNA. The signal intensity was amplified by second staining with biotin labeled anti-streptavidin antibody followed by phycoerythrin- streptavidin staining. Fluorescent images were captured using Hewlett-Packard G2500A gene Array Scanner. All of the arrays used in the study passed the quality control set by Tumor analysis group 2004.[22]

Data Analysis

Initial data analysis of Affymetrix microarrays was done using Genechip GX software (version 7.3.1), with standard operating procedures and quality controls as described previously (Tumor analysis group 2004).[22] Normalized signals (expression values) were calculated using three probe set algorithms, DNA-Chip Analyzer 1.7 model based expression (dChip/mismatch model),[23] Microarray Suite 5 (MAS5) (Affymetrix) probe set algorithms, and Probe Logarithmic Intensity Error, SDK Version 2 (PLIER) (Affymetrix). We have previously reported that PLIER and dCHIP difference model probe set algorithms provide a good signal/noise ratio in human muscle expression profiling projects,[24,25] and we also added MAS5 probe set algorithm as this remains the most commonly used. CEL processed image files were analyzed separately for MAS5, dCHIP, and PLIER probe set algorithms. For the study of molecular markers of inflammatory cell subsets and activation states, and for analysis of transcripts previously reported as differentially regulated, a candidate gene approach was used (See Supplemental Table S1 at *http://ajp.amjpathol.org*). For non-candidate (global) analysis approaches, we used concordance for three probe set algorithms and a relatively stringent P value threshold ($P < 0.005$) for each of the three probe set algorithms.

Immunohistochemistry Analysis

Muscle biopsies selected for protein validation studies included a subset of those used for microarray studies (dysferlin-deficient, FKRP [LGMD2I]), as well as additional biopsies from Becker muscular dystrophy, Juvenile Dermatomyositis patients and for normal controls that showed no histological or biochemical abnormality. Serial 6 μm-thick frozen muscle sections were cut with an IEC Minotome cryostat, mounted to Superfrost Plus Slides (Fisher Scientific Pittsburgh, PA). Sections were then blocked for 30 minutes in 10% horse serum and 1× PBS and incubated with respective antibodies for 2 hours at room temperature. Mouse monoclonal antibody against versican (US Biological Swampscott, MA) and tenascin-C (Sigma St. Louis, MO) at the 1:1500 dilutions and myoferlin at 1:20 dilutions were used.[26] Antibodies used included a rabbit polyclonal antibody against Rab27A (IBL, Japan) at the concentration of 2 μg/ml along, a mouse monoclonal antibody against laminin α 2 (Chemicon, CA) at 1:500, and a mouse monoclonal antibody against HLA-DR (DakoCytomation, CA) at 1:50. Washes were done with 10% horse serum and 1× PBS and sections were then incubated with respective secondary antibody, Cy3 and Cy2 conjugated goat anti-mouse antibody and Cy3 conjugated donkey anti-rabbit (Jackson Immunoresearch Inc. Westgrove, PA) at a 1:500 dilution. Isotype-matched mouse and rabbit Igs were used instead of primary antibodies as negative controls.

Confocal images were captured on the inverted Olympus microscope equipped with a ×40 (DApo 40UV/340: NA 1.30) or ×60 (Splan Apo; NA 1.4) objective lens, Bio-rad confocal hardware (Bio-rad MRC 1024 ES, Bio-rad Hercules, CA), and a 15mW air-cooled Cr/Ar laser for excitation. Cy3 and Cy2 were detected using standard protocols for Cy3 and Cy2 antibody respectively.

Immunoblot Analysis

Biopsy cryosections were solubilized with 100 μl JSB buffer (0.1 M Tris pH 8.0, 10% SDS, 50 mmol/L DTT, 10 mmol/L EDTA, pH 8.0, and 0.02% bromophenol blue). The lysate was boiled for 5 minutes and then centrifuged at 13,000 × g at 4°C for 5 minutes. Ten microliters of each supernatant was run on a ready-cast 4% to 15% Tris-HCl

polyacrylamide gel (Biorad) with protein markers (Kaleidoscope Precision Plus protein standard, Biorad, CA). Samples were then transferred onto Hybond C Extra membrane (Amersham, Little Chalfont, UK), blots blocked in 5% milk in Tris- buffered saline with 0.5% Tween 20, and then incubated with primary antibodies (below), and horseradish peroxidase-conjugated secondary antibodies. Slp2a-SHD antibody was affinity-purified rabbit IgG, used at 2 μg/ml concentration for immunoblot.[27] Rab27A antibody was also affinity purified rabbit IgG and used at 5 μg/ml concentration for immunoblot. Myoferlin immunoblotting was done using a mouse monoclonal supernatant[26] at dilution of 1:50. Dysferlin immunoblotting was done with a mouse monoclonal at a dilution of 1:200 (NCL-Hamlet-2, Novocastra). After incubation three washes with TBST followed by incubation in respective horseradish peroxidase-conjugated secondary antibodies (Biorad). Detection of protein bands was performed using ECL detection kit (Amersham) and Hyperfilm ECL (Amersham) X-ray film.

Results

Biochemical and Genetic Characterization of LGMD Patient Biopsies

We characterized a series of LGMD patient muscle biopsies at both the biochemical and genetic level, with the goal of defining molecular networks specific to dysferlin-deficient muscle (LGMD2B or MM). Twenty-five subjects showing complete or partial dysferlin deficiency by immunoblot analyses of muscle biopsies were studied for dysferlin gene mutations (Table 1). Genomic DNA was isolated from each biopsy and tested for mutations of all 55 exons of the dysferlin gene using denaturing high-pressure liquid chromatography and sequencing. Nineteen of the 25 subjects studied tested positive for gene mutations (Table 1). Out of these 19 mutation-positive patients, two patients were homozygous, nine (47%) were compound heterozygotes, and in eight patients we were able to detect only one mutation. In all, 26 distinct sequence variants were identified and 13 (50%) were novel to this report.

For LGMD2I patients, approximately 1000 muscle biopsies were first tested for the common mutation in FKRP gene [*c.826C>A (p.Leu276Ile)*] using a Taqman allele discrimination assay (Table 1). Sixteen patients showed heterozygosity for common mutation and ten were homozygous. Heterozygotes were then subjected to coding region DNA sequencing, and five compound heterozygotes identified. Of these, nine mutation-positive patient muscle biopsies were used for mRNA profiling and protein studies (Table 1).

mRNA Profiling Shows Most Transcriptional Changes to be Shared between LGMD2B and LGMD2I

We used mRNA profiling of 54,000 probe sets in patient muscle biopsies from LGMD2B/MM (dysferlin deficiency; $n = 10$), LGMD2I (FKRP deficiency; $n = 9$), ALS ($n = 7$), and normal volunteers ($n = 11$) using the HG-U133 Plus 2.0 microarrays (Affymetrix). To interpret the microarray data, we used multiple probe set algorithms (MAS5.0, dCHIP difference model, PLIER).

Initial data analysis was done focusing on candidate genes or proteins, previously reported as aberrantly expressed in dysferlin-deficient muscle from either human patients, or mouse models (Figure 1A).[28–32] Fourteen probe sets corresponding to full length transcripts from 10 genes were queried in dysferlin-deficient, FKRP-deficient and normal control muscle biopsies. Seven of the 10 previously reported transcripts genes showed similar expression in dysferlin- and FKRP-deficient muscle (Figure 1A). These data suggest that many of the previously reported differentially expressed genes in dysferlin-deficient muscle are shared with other dystrophies, and likely reflective of general muscle pathology rather than biochemical pathways directly related to dysferlin-deficiency.

We validated and extended previously reported data on three genes: Fer1L3 (myoferlin), S100A11, and Calpain 3. The FER-1 family member, Fer1L3 (also called myoferlin), and S100A11 showed increased mRNA levels in LGMD2I patients, but significantly higher expression in LGMD2B.[30] Calpain 3 has been previously reported as showing decreased protein expression in dysferlin-deficient patient biopsies.[33] We extended this data, showing LGMD2B disease-specific reductions in Calpain 3 mRNA (Figure 1A).

Fer1L3 (myoferlin) has been proposed to show compensatory up-regulation in dysferlin-deficient muscle. In our series here, myoferlin was highly up-regulated in both LGMD2I and dysferlin-deficient muscle, although it was significantly higher in dysferlin-deficient patient muscle (Figure 1A). We validated this finding using immunostaining and immunoblotting of myoferlin (See Supplement Figure S1 at *http://ajp.amjpathol.org*). Myoferlin expression was quite variable from biopsy to biopsy, and was most increased in a dysferlin-deficient muscle showing considerable fibrofatty replacement (patient D5, See Supplement Figure S1A at *http://ajp.amjpathol.org*). By immunostaining, myoferlin protein expression was strongly expressed on all myofibers and blood vessels (veins, arteries, and capillaries), as well as increased staining in perimysial connective tissue (See Supplement Figure S1B *http://ajp.amjpathol.org*). Myoferlin is considered a developmental isoform in muscle (myoblast/myotube fusion), but we found myoferlin to be expressed in all myofibers in both dysferlin deficiency and FKRP [LGMD2I] patients, and not limited to regenerating fibers.

mRNA Profiling, Identifies Disease-Specific Abnormalities in Dysferlin-Deficiency

To identify differentially expressed genes specific for dysferlin deficient patients (LGMD2B and MM), we used a two tiered approach for the analysis of the expression profiles. First, we compared a combined normal and disease control group of profiles (normal volunteers, ALS, and FKRP [LGMD2I]; $n = 27$) with dysferlin deficient

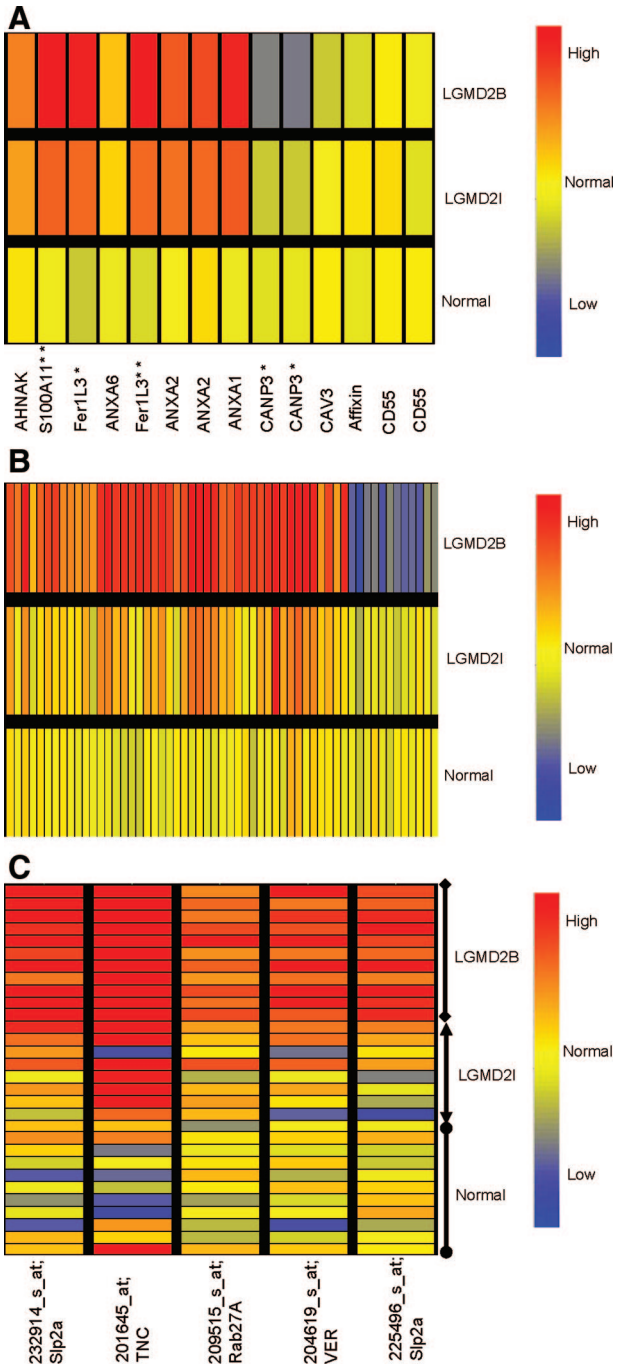

Figure 1. mRNA Profiling Identifies both Pathology-Associated and Dysferlin-Specific Transcription Changes. **A:** Shown is relative expression of transcripts previously reported to be associated with dysferlin-deficiency.[22–25] Signals (PLIER) from patients muscle biopsies were averaged, and normal volunteer muscle (Normal; $n = 11$), FKRP muscle (LGMD2I; $n = 9$), and Dysferlin-deficient (LGMD2B; $n = 10$). Some transcripts showed multiple probe sets against the full-length transcript, and in these cases results for both probe sets are shown (ANXA2 [annexin 2], CANP3 [calpain 3], CD55 [DAF]). Most transcripts (7/10 genes) showed similar expression pattern in FKRP and dysferlin-deficient patient biopsies. Myoferlin [Fer1L3], and S100A11 were increased in both FKRP and dysferlin deficiency, although increases were higher in dysferlin (*$P < 0.05$; **$P < 0.01$). Calpain 3 mRNA was specifically reduced in dysferlin-deficient muscle, as previously reported (*$P < 0.05$).[33] Red color indicates increased expression of the mRNA, while blue indicates decreased expression. **B:** Shown are statistically significant altered transcripts specific for dysferlin-deficiency (Welch analysis of variance $P < 0.005$). Signals (PLIER) from patients muscle biopsies were averaged and represented. Fifty-eight differentially expressed genes specific for dysferlin deficient group were observed (see Table 2 for P values and fold changes). **C:** Shown are signals for the transcripts specific to dysferlin-deficient muscle that were validated by protein studies. Multiple probe sets for Slp2a are shown, and each individual patient signal represented separately. Transcripts for an alternative vesicle trafficking pathway, Synaptotagmin-like protein (Slp2a) and a small GTPase (Rab27A) were significantly higher in all dysferlin deficient patients. Two inflammatory proteins, tenascin (TNC) and versican (VER) were found highly expressed in dysferlin-deficient muscle sample at mRNA level compared with FKRP and normal samples.

profiles ($n = 10$). Probe sets with analysis of variance $P < 0.01$ for each of three distinct probe set algorithms (dCHIP difference model, PLIER, MAS5.0) were retained. Nine hundred and twenty two (922) genes were differentially expressed in the dysferlin-deficient group by this analysis. This initial tier of analysis was done to filter out probe sets that showed high variation between human muscle biopsies. As a second tier, we then created a two group dataset (LGMD2B $n = 10$; LGMD2I $n = 9$), and retained those transcripts from the 922 that showed analysis of variance $P < 0.005$ for one or more probe set algorithms, and 271 of the 922 survived this stringent statistical filter for disease-specificity for one probe set algorithm, and 58 of the 271 (21%) were concordant for all three algorithms. A description of each of the 58 probe sets is provided (Table 2). Graphical representation of these 58 probe sets is shown in the heat map in Figure 1B. Of these, 21% showed lower mRNA levels in LGMD2B, and 79% showed increased levels.

Disease-Specific Induction of Slp2a and Rab27A Suggest Compensatory Vesicle Trafficking Pathway

The 58 dysferlin-deficient-specific transcripts were queried to affirm that they detected the canonical full-length transcripts (non-intronic), and for potential functional significance in muscle vesicle trafficking or inflammation. With regards to membrane and vesicle trafficking, two proteins were particularly interesting; Rab27A and Slp2a. Both were increased in all dysferlin-deficient patients, yet were not increased in any control or FKRP [LGMD2I] patient biopsy (Figure 1C).

The Rab proteins are a family of over 60 genes that encode small GTP-binding proteins involved in intracellular membrane traffic, and each works in concert with a protein binding partner (effector) that bind to activated (GTP-bound) Rab forms. Rab27A has been well-studied as mutations result in an immune deficiency genetic disorder (Griselli Syndrome type II), and Rab27-binding effectors are members of the synaptotagmin-like family (Slp).[34] The two genes identified in our dysferlin-specific profiles, Rab27A and Slp2a, have been shown to directly interact in melanosome traffic in melanocytes.[27,35]

We hypothesized that the increased levels of Rab27A and Slp2 seen in dysferlin-deficient muscle could represent compensatory up-regulation of an alternative vesicle trafficking pathway. To test this, we examined the protein expression of Rab27A in normal controls, dysferlin-deficient, LGMD2I and Becker dystrophy patient muscle biopsies by immunostaining (Figure 2). Co-staining with laminin $\alpha 2$ (merosin) was

Table 2. Table Showing Fifty-Eight Differentially Expressed Genes Specific for Dysferlin Deficient Group with their Respective *P* Value and Fold Change from PLIER

Probe set	*P* value	Fold change	Gene Symbol	Description
233696_at*	<0.001	−1.97	VPS37C	Vacuolar protein sorting 37 homolog C (*S. cerevisiae*)
210251_s_at	<0.001	2.91	RUFY3	RUN and FYVE domain containing 3
213457_at	<0.001	3.48	MFHAS1	Malignant fibrous histiocytoma amplified sequence 1
211551_at	<0.001	−2.29	EGFR	Epidermal growth factor receptor
227812_at	<0.001	3.17	TNFRSF19	Tumor necrosis factor receptor superfamily, member 19
205640_at	<0.001	6.86	ALDH3B1	Aldehyde dehydrogenase 3 family
227798_at	<0.001	1.60	SMAD1	SMAD, mothers against DPP homolog 1 (Drosophila)
219517_at	<0.001	2.66	ELL3	Elongation factor RNA polymerase II-like 3
209515_s_at	<0.001	3.06	RAB27A	RAB27A, member RAS oncogene family
36030_at	<0.001	2.11	HOM-TES-103	Hypothetical protein LOC25900
209211_at	<0.001	3.00	KLF5	Kruppel-like factor 5 (intestinal)
216609_at	<0.001	3.20	TXN	Thioredoxin
200772_x_at	<0.001	2.04	PTMA	Prothymosin, alpha (gene sequence 28)
204736_s_at	<0.001	4.08	CSPG4	Chondroitin sulfate proteoglycan 4
209212_s_at	<0.001	2.42	KLF5	Kruppel-like factor 5 (intestinal)
218691_s_at	<0.001	3.39	PDLIM4	PDZ and LIM domain 4
216294_s_at	<0.001	−2.21	KIAA1109	KIAA1109
222288_at	<0.001	3.20	NK	Transcribed locus
211921_x_at	0.001	2.15	PTMA	Prothymosin, alpha (gene sequence 28)
209360_s_at	0.001	4.34	RUNX1	Runt-related transcription factor 1 (acute myeloid leukemia 1)
1552263_at	0.001	2.76	MAPK1	Mitogen-activated protein kinase 1
225188_at	0.001	2.42	RAPH1	Ras association and pleckstrin homology domains 1
203186_s_at	0.001	2.26	S100A4	S100 calcium binding protein A4
221765_at	0.001	3.44	UGCG	UDP-glucose ceramide glucosyltransferase
216791_at	0.001	−1.77	TMEM92	Transmembrane protein 92
225852_at	0.001	1.48	ANKRD17	Ankyrin repeat domain 17
205478_at	0.001	−2.59	PPP1R1A	Protein phosphatase 1, regulatory (inhibitor) subunit 1A
223538_at	0.001	1.65	SERF1A	Small EDRK-rich factor 1A (telomeric)
212295_s_at	0.001	2.04	SLC7A1	Solute carrier family 7, member 1
227253_at	0.001	2.84	CP; HPS3	Ceruloplasmin (ferroxidase)
238013_at	0.001	4.11	PLEKHA2	Pleckstrin homology domain containing
209169_at	0.001	2.66	GPM6B	Glycoprotein M6B;
235981_at	0.001	−3.03	C8orf22	Chromosome 8 open reading frame 22
211503_s_at	0.001	1.52	RAB14	RAB14, member RAS oncogene family
225496_s_at	0.001	2.99	SYTL2/Slp2a	Synaptotagmin-like 2; synonyms: SLP2,
238909_at	0.001	2.04	S100A10	S100 calcium binding protein A10
201645_at	0.001	6.41	TNC	Tenascin C (hexabrachion)
1554513_s_at	0.002	1.47	CCDC123	Coiled-coil domain containing 123
206714_at	0.002	−1.73	ALOX15B	Arachidonate 15-lipoxygenase, type B
225189_s_at	0.002	2.16	RAPH1	Ras association and pleckstrin homology domains 1
204619_s_at	0.003	2.64	CSPG2	Chondroitin sulfate proteoglycan 2 (versican)
222876_s_at	0.003	2.33	CENTA2	Centaurin, alpha 2
211862_x_at	0.003	−1.56	CFLAR	CASP8 and FADD-like apoptosis regulator
243794_at	0.003	−2.13	NK	Transcribed locus
224563_at	0.003	2.96	WASF2	WAS protein family, member 2
236304_at	0.003	2.70	NK	Transcribed locus
217040_x_at	0.003	−1.76	SOX15	SRY (sex determining region Y)-box 15
201291_s_at	0.003	4.28	TOP2A	Topoisomerase (DNA) II alpha 170kDa
217728_at	0.003	2.11	S100A6	S100 calcium binding protein A6
208485_x_at	0.003	−1.57	CFLAR	CASP8 and FADD-like apoptosis regulator
231712_at	0.003	2.41	NK	Transcribed locus, strongly similar to XP_525018.1
227595_at	0.003	1.45	ZMYM6	zinc finger, MYM-type 6
225997_at	0.004	1.88	MOBKL1A	MOB1, Mps One Binder kinase activator-like 1A (yeast)
232914_s_at	0.004	2.33	SYTL2/Slp2a	Synaptotagmin-like 2; synonyms: SLP2,
206460_at	0.004	−2.30	AJAP1	Adherens junction associated protein 1
1552455_at	0.004	2.74	C9orf65	Chromosome 9 open reading frame 65
227568_at	0.004	2.00	HECTD2	HECT domain containing 2
222834_s_at	0.005	2.04	GNG12	Guanine nucleotide binding protein (G protein), gamma 12

*This probe corresponds to one of the small EST in VPS37C gene, NK, Not known.

performed (Figure 2). No detectable protein expression of Rab27A was observed in normal biopsies (n = 3), LGMD2I (n = 3) and Becker dystrophy (n = 3) patients. Dysferlin-deficient biopsies (n = 6) all showed detectable Rab27A immunostaining. Rab27A staining was evident within myofibers, typically as a punctate staining pattern distributed throughout the cytoplasm. The staining intensity was variable, with a mosaic pattern of some myofibers showing very high levels and others low levels (see patient D10; Figure 2), while in other biopsies the majority of myofibers showed increased staining signal (see patient D1, D3 Figure 2).

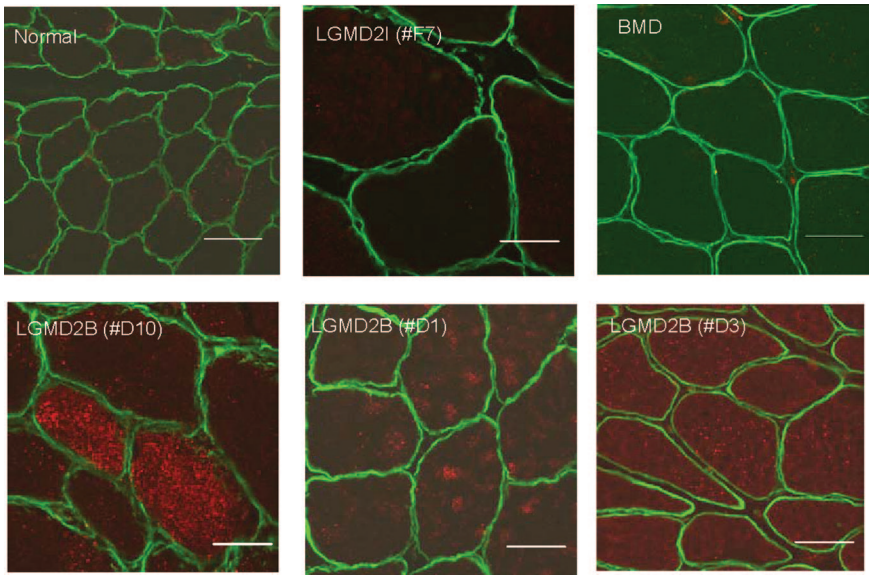

Figure 2. Rab27A Immunostaining in Muscle Biopsies. Shown are confocal images of Rab27A (red) and merosin (laminin α2) (green) co-stained in patient muscle biopsies. Dysferlin-deficient patient muscle (LGMD2B) showed high-level but variable expression of Rab27A in myofibers. In LGMD2B Patient #D10, a subset of myofibers showed high level Rab27A expression. In Patients #D1 and #D3, Rab27A was seen at lower levels in the majority of fibers. Rab27A signal was not detectable in normal controls, LGMD2I, or Becker muscular dystrophy. Scale bar = 50 μm.

To provide more quantitative assessments of Rab27A expression, immunoblotting was done in dysferlin-deficient samples (n = 4) compared to FKRP (n = 3) and normal controls (n = 2) (Figure 3A). Quantitation of level of Rab27A (55kDa) relative to two different control proteins was done (myosin post-transfer staining, and β-tubulin immunoblotting on same membrane). This analysis showed that Rab27A is significantly increased in dysferlin-deficient muscle relative to both normal and disease controls (Figure 3, B and C).

LGMD2B patient biopsies can show more inflammatory infiltrates than FKRP (LGMD2I). To determine whether Rab27A protein expression was co-localized with inflammatory cells, we co-stained for Rab27A and HLA-DR (macrophages) in both LGMD2B and Juvenile Dermatomyositis muscle biopsies. This analysis showed distinct localization of the two antibodies, with lower myofiber expression of Rab27A in Juvenile Dermatomyostis, consistent with the immunostaining and immunoblotting above (See Supplement Figure S2 at *http://ajp.amjpathol.org*).

We then tested for levels of Slp2a protein. Antibody for Slp2a detected the expected 110kDa protein by immunoblotting in all six dysferlin-deficient patients tested but no expression was detected in each of the normal controls (n = 4) or FKRP (LGMD2I; n = 4) patient muscles (Figure 4).

Rab27A is known to form a complex with a motor protein, non-muscle myosin 5A (MYO5A) through direct interaction with MYO5A receptor Slac2-a/melanophilin.[36,37] The MYO5A transcript was not identified as differentially expressed in our initial highly stringent list of transcripts specific for dysferlin deficient muscle (Table 2). However, query of probe sets for MYO5A in the PLIER data showed significantly increased MYO5A transcript levels in dysferlin-deficient muscle compared to FKRP [LGMD2I] (P = 0.016).

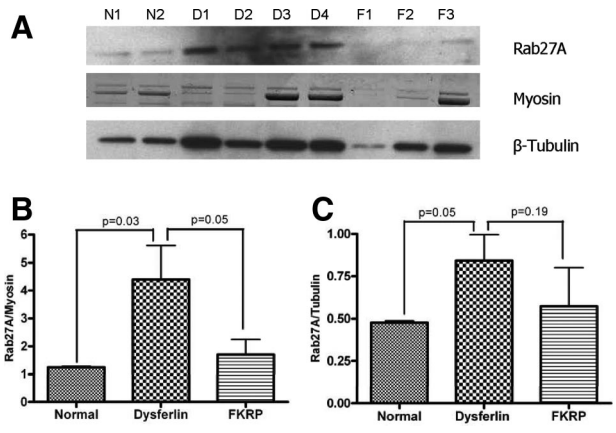

Figure 3. Quantitation of Rab27A in Muscle (**A**) shows immunoblot for Rab27A (~55kDa) in patient muscle biopsies. Low levels of Rab27A protein is seen in normal control muscle (N1 and N2) and in FKRP dystrophy muscle (LGMD2I) (F1, F2 and F3) muscle, whereas dysferlin deficient patient muscle (D1, D2, D3 and D4) shows increased Rab27A protein. Rab27A protein expression levels were calculated as ratios relative to two control proteins; myosin heavy chain Coomassie Blue staining (**B**), and β-tubulin immunoblot (**C**).

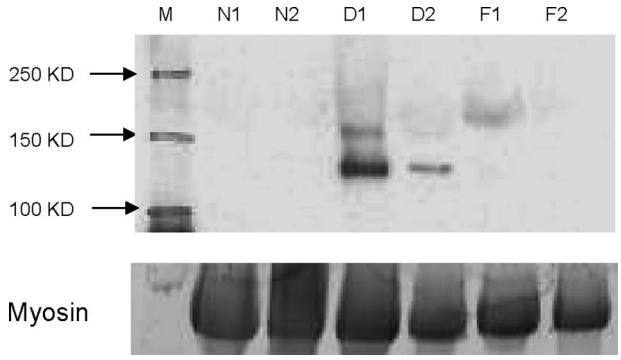

Figure 4. Dysferlin-Deficient Muscle Shows Disease-Specific Increase in Slp2a Protein. Shown is an immunoblot developed for the detection of Slp2a (~110kd) using Slp2a-SHD antibody. Shown are muscle containing no detectable Slp2a protein in normal (N1 and N2) and in [LGMD2I] FKRP (F1 and F2) patients, whereas dysferlin deficient patients (D1 and D2) show Slp2a of the expected molecular weight (m). Shown below is myosin in the post transfer gel to control for loading of muscle proteins.

Inflammatory Changes in LGMD2B

LGMD2B patients can show an inflammatory onset, and can be misdiagnosed as polymyositis. We queried the profiles for proteins well characterized and specific for T cells (CD2, CD4, CD3E, CD28, CD45, CD152), tissue dendritic cells (CD8a, CD83, CD86), B cells (CD19, CD22), and macrophage activation markers (23 transcripts; see Supplemental Table S1, at *http://ajp.amjpathol.org*). This showed that the majority of marker transcripts were strongly elevated in the two dystrophies relative to normal control muscle, but similarly expressed between LGMD2I and LGMD2B (Figure 5; See Supplemental Table S1 at *http://ajp.amjpathol.org*). B cell and dendritic cell markers showed no significant differences.

There were three T cell markers that were significantly different between LGMD2B (dysferlin) and LGMD2I (FRKP); CD28 and CD45 (PTPRC) were increased in LGMD2B, and CD152 (CTLA4) decreased (Figure 5A). Both CD28 and CD152 are co-stimulatory molecules expressed by activated T cells, where both bind to (CD80) and (CD86 at different affinities).[38] However, CD28 transmits a stimulatory signal, while CD152 (CTLA4) transmits an inhibitory signal. Our finding of a significantly increased stimulatory signal (CD28) and significantly decreased inhibitory signal (CD152) indicates a high state of activation of T cells in dysferlin-deficient muscle.

We also found four activated macrophage markers significantly increased in dysferlin-deficient muscle (LCP2, RAD1, ANXA4, S100A13), and one marker decreased (RAC1) (Figure 5B). Most of these markers are involved in membrane remodeling, and may be reflective of altered vesicle traffic.

We also searched our stringent global data set concordant for all three probe set algorithms for inflammation-associated transcripts. Two extracellular matrix markers of inflammation, tenascin-C and versican, were up-regulated in both dystrophies, but significantly higher in dysferlin-deficient muscle (Figure 1C). To validate the microarray data and to examine the tissue localization of tenascin-C (A, B, C) and versican (D, E, F) we performed immunostaining on patient muscle biopsies (Figure 5C). Both proteins showed similar localization in endomysial connective tissue and blood vessels. Normal control muscles ($n = 6$) showed relatively rare punctate staining, often near capillaries. Both FKRP [LGMD2I] ($n = 6$) and dysferlin-deficient muscle [LGMD2B] ($n = 6$) showed a marked increase in immunostaining, with extensive labeling of the endomysial connective tissue, with increased intensity around all myofibers, likely at or near the basal lamina. Immunostaining was considerably more intense in dysferlin-deficient muscle compared to LGMD2I (Figure 5C), consistent with the microarray mRNA data.

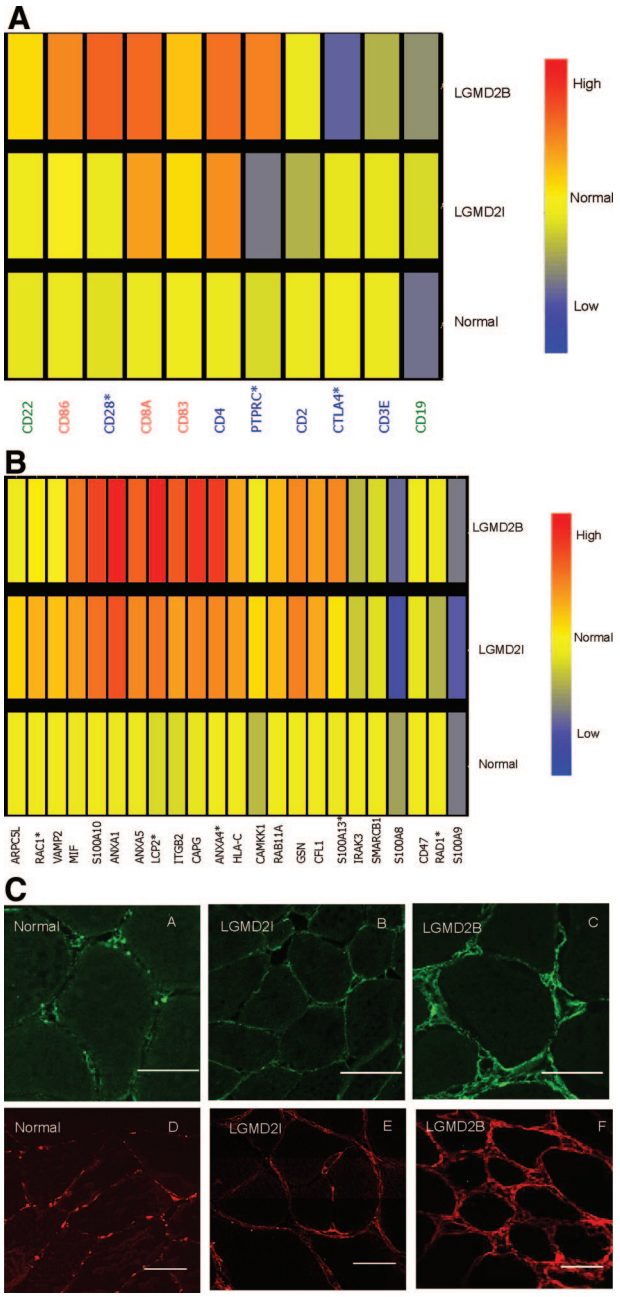

Figure 5. Inflammation Related Transcripts in Muscle. **A:** Shows candidate mRNA markers for T cells (blue font), B cells (green), and dendritic cells (red) queried against the muscle biopsy mRNA profiling data set, showing average expression levels for each group. Two T cell activation markers were increased in dysferlin deficiency (*$P < 0.05$) relative to FKRP dystrophy (CD28, PTPRC), and one T cell co-stimulatory suppression marker was decreased (CTLA4). This suggests an increase in the T cell costimulatory activity in LGMD2B muscle. **B:** Shows candidate mRNA markers for macrophages. Five transcripts were significantly altered in transcription (*$P < 0.05$), with four of these significantly increased in LGMD2B (LCP2, RAD1, ANXA4, and S100A13). **C:** Shows immunostaining for tenascin C (A, B, C) and versican (D, E, F) in muscle biopsies. Frozen sections were from normal control, FKRP [LGMD2I] (≠F7), and dysferlin-deficient mutation positive patient (≠D10). Tenascin-C is expressed at the plasma membrane, extracellular matrix, and blood vessels at a higher level in dysferlin-deficient muscle compared to FKRP biopsies. In normal muscle, tenascin-C shows low level patchy immunostaining at the plasma membrane. Confocal imaging of versican shown in normal control, LGMD2I and dysferlin deficient patients shows a pattern similar to tenascin-C, with increased staining in dysferlin-deficient muscle. Scale bar, 50 μm.

Discussion

We used mRNA profiling to define inflammatory and vesicle trafficking alterations in muscle that were specific to dysferlin-deficiency (LGMD2B/MM). Mutation-positive LGMD2B/MM patients, disease controls ([LGMD2I] FKRP;

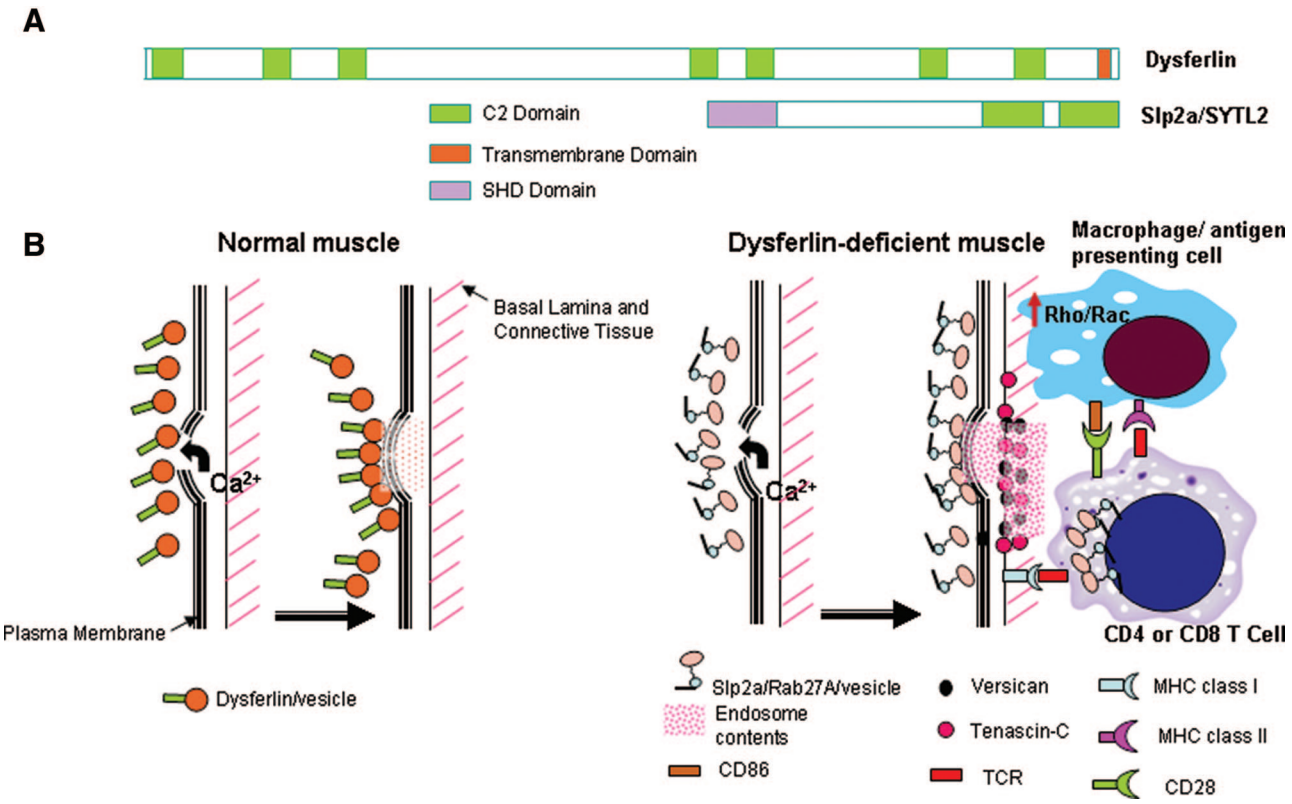

Figure 6. Model for Effective Compensatory Membrane Repair, but Proinflammatory Milieu in Dysferlin Deficient Muscle. **A:** Shown is the dysferlin protein (230kDa) with seven putative C2 domains and a C-terminal transmembrane domain (TM), compared to the Slp2a/SYTL2 protein (110kDa) containing two C2 domains. Slp2a contains an extra SHD domain, that is absent in dysferlin. The SHD domain is important for binding GTP-bound activated form of Rab proteins on vesicles, where the complex then participates in vesicle trafficking pathways. Protein schematics are drawn to relative scale. **B:** Shown is a schematic of plasma membrane repair in normal muscle following membrane damage, and a model of consequences of compensatory up-regulation of the Slp2a/Rab27A pathway. In normal myofibers, dysferlin plays a major role in vesicle traffic and membrane repair in response to calcium influx. In dysferlin-deficient myofibers, the Slp2a/Rab27A complex is highly expressed, presumably to compensate for lack of dysferlin-linked membrane repair mechanisms. This may effectively repair myofiber membrane damage and no symptoms for two decades. We hypothesize that four interrelated processes may combine to drive disease onset and progression: 1) release of Slp2a/Rab27A exocytotic vesicle contents (pink diamonds); 2) increased Rho/Rac signaling in dysferlin-deficient macrophages lead to activation and inappropriate phagocytotic activity; 3) possible positive feedback between the T cell Slp2a/Rab27A-mediated lytic granule cell killing, and up-regulated Slp2a/Rab27A; and 4) possible interaction between activated macrophages/dendritic cells with CD4 T cells via signal 1 (MHC class II and CD4) and signal 2 (CD86 and CD28) as well as interaction between CD8 T cells and MHC class I on muscle lead to further immune activation. The observed focal increases in versican and tenascin-C may contribute to, or simply reflect the pro-inflammatory milieu.

ALS), and normal volunteers (control) were studied for profiling and/or protein validations. We analyzed the mRNA profiling data set using three complementary approaches: candidate gene queries of previously reported profiling studies in LGMD2B (mouse or human), query of well-characterized markers of inflammatory cell subtypes (B cell, T cell, dendritic cell, and macrophage), and a stringent global approach (concordance for three probe set algorithms, each $P < 0.005$). Analysis of microarray data sets is heavily influenced by the choice of probe set algorithm, with only about 30% concordance between different analysis methods,[25] and we have previously reported the stringent concordance method as a highly specific but less sensitive approach to complex data sets.[39] Importantly, our global approach identified a compensatory vesicle trafficking pathway not previously reported in muscle (Rab27A/Slp2a) as specifically increased in dysferlin-deficient muscle (Figures 2, 3, 4).

Rab27A is a member of the Rab family of small GTP-binding proteins, and many of the members have been shown to control intracellular membrane trafficking in eukaryotic cells.[34] In melanocytes, Rab27A, together with Slp2a, has been shown to be involved in the control of melanosome transport, especially at the anchoring of melanosomes to the plasma membrane.[35] In cytotoxic T lymphocytes, Rab27A participates in lytic granule exocytosis.[40] Rab27A effector Slp2a also mediates tight docking of mucus granules onto apical plasma membrane of gastric surface mucous cells.[41]

Rab27A, like other Rab family members, directly interacts with membranes and vesicles via covalent attachment to lipid (prenylation), and then requires effector proteins bound to their N-terminal SHD-domains to dictate what downstream action is to be taken with the vesicle (transport, fusion, exocytosis, etc). Rab27A has multiple effector proteins in different cell types,[34] however Slp2a, a member of the synaptotagmin like protein family, has been shown to be the Rab27A effector for melanosome transport in melanocytes.[27,35]

We found Slp2a to be induced in dysferlin deficient muscle, and like Rab27A, was a disease-specific finding. Synaptotagmins are structurally related to dysferlin, where both contain multiple C2 domains, and both function as Ca^{2+} sensors in the process of vesicular trafficking

and exocytosis (Figure 6A). Thus, it is likely that Rab27A and Slp2a are binding partners in dysferlin-deficient muscle, and are functioning as a compensatory vesicle trafficking pathway. Myoferlin, a C2-containing protein very closely related to dysferlin, was also strongly induced in dysferlin-deficient muscles around all myofibers (See Supplement Figure S1 at *http://ajp.amjpathol.org*). However, this was not disease-specific, as FKRP patient muscle also showed strong upregulation around all fibers. Nevertheless, myoferlin may participate with Rab27A/Slp2a in providing compensatory membrane repair in dysferlin-deficient muscle.

Patients with mutations in the Rab27A gene show Griscelli syndrome, an autosomal recessive disorder with a failure of cytotoxic T cell killing caused by the defect in cytolytic granule exocytosis.[42] In CTLs derived from type II Griscelli syndrome patients, lytic vesicles appear to retain the ability to polarize toward the target cells but they are unable to dock to the plasma membrane and unable to kill target cells, suggesting that Rab27A is involved in the late stage of membrane fusion and granule release.[43] We have shown disease-specific increase in Rab27A expression on dysferlin-deficient muscle fibers, and it is tempting to hypothesize that the aberrant expression of Rab27A may cause over-stimulation of immune cells. Another possibility is that the vesicles trafficked by Rab27A/Slp2a may hold lysosomal contents that, when release by dysferlin-deficient fibers, cause excessive stimulation of lymphocytes and macrophages. Two genes can cause Griscelli syndrome, Rab27A, and MYO5A.[44] MYO5A is a non-muscle myosin motor protein that provides a scaffold on which to transport vesicles containing Rab27A, and mutations of either MYO5A or Rab27A lead to the same defect in vesicle fusion. Interestingly, the mRNA corresponding to MYO5A was significantly increased in dysferlin-deficient muscle compared to LGMD2I muscle.

The data presented in this report, taken together with the recently reported functional studies of dysferlin-deficient monocytes/macrophages,[18] lays the foundation for a model that may explain molecular mechanism of the subacute inflammatory onset of LGMD2B/MM. In normal muscle, dysferlin participates in calcium-sensitive vesicle traffic and membrane repair (Figure 6B). In dysferlin-deficient muscle, this vesicle pathway is lost, and this leads to compensatory up-regulation of an alternative vesicle traffic pathway involving a C2-domain containing protein related to dysferlin, Slp2a, and its binding partner Rab27A (Figure 6B). We hypothesize that the Slp2a/Rab27A pathway, possibly in concert with the up-regulated myoferlin pathways, is able to effectively perform calcium-mediated membrane repair in dysferlin-deficient muscle. These compensatory pathways rescue muscle function, and permit patients to remain asymptomatic until their late teens or early 20s.

Muscle pathology, presentation, and disease progression may be related to three interconnected microenvironmental changes in dysferlin-deficient muscle that occur later and may be associated with muscle damage. First, the Slp2a/Rab27A pathway is an endocytotic/exocytotic pathway, and it may repair membrane damage but then release vesicular contents to the extracellular space (Figure 6B). This may lead to perturbed growth factor and cytokine milieu. Second, LGMD2B patient muscle macrophages are themselves dysferlin-deficient, and these cells have been shown to overstimulate rho/rac signaling, and show abnormally high phagocytotic activity[18] (Figure 6B). Third, infiltrating T cells are known to rely on the Rab27A/Slp2a/MYO5A vesicle pathway for lytic granule fusion and cell killing, and the aberrant release of Rab27A/Slp2a vesicles by myofibers may inappropriately signal CD8 T cell killing of MHC class I expressing myofibers. The combination of these three factors may lead to a pro-inflammatory milieu, culminating in immune cell mediated myofiber damage. This model may explain the strong focal increases of versican and tenascin-C seen in dysferlin-deficient muscle (Figure 6).

The inflammatory infiltrate in dysferlin deficient muscle consists of macrophages, dendritic cells, and CD4 and CD8 T cells.[14,38] We found increase in costimulatory markers (increase in CD86 on dendritic cell, increase in CD28 and decrease in inhibitory CD152 [CTLA4] on T cells) suggesting a skewed T cell activation in dysferlin deficient muscle (Figure 5A; Supplementary Table S1 at *http://ajp.amjpathol.org*). Tenascin and versican are known to bind and immobilize growth factors in the tissue micromilieu, thereby protecting them from proteolytic cleavage and facilitating presentation to appropriate cell surface receptors. Thus, both proteins facilitate the inflammatory process, while recruiting cell types involved in wound repair and fibrosis, such as myofibroblasts. We hypothesize that the increased rho signaling in macrophages, altered costimulatory pathways leading to activation of T cells within the muscle, and the disease-specific alteration of the tissue microenvironment combine to drive the inflammatory onset of LGMD2B.

Acknowledgments

We thank Dr. Anastas Popratiloff of the George Washington University MRDDRC Imaging Core for assistance with confocal microscopy and Eiko Kanno from Tohoku University for assisting with Slp2a antibody preparation.

References

1. Bonnemann CG, McNally EM, Kunkel LM: Beyond dystrophin: current progress in the muscular dystrophies. Curr Opin Pediatr 1996, 8:569–582
2. Liu J, Aoki M, Illa I, Wu C, Fardeau M, Angelini C, Serrano C, Urtizberea JA, Hentati F, Hamida MB, Bohlega S, Culper EJ, Amato AA, Bossie K, Oeltjen J, Bejaoui K, McKenna-Yasek D, Hosler BA, Schurr E, Arahata K, de Jong PJ, Brown RH Jr: Dysferlin, a novel skeletal muscle gene, is mutated in Miyoshi myopathy and limb girdle muscular dystrophy. Nat Genet 1998, 20:31–36
3. Han R, Campbell KP: Dysferlin and muscle membrane repair. Curr Opin Cell Biol 2007, 19:409–416
4. Saito A, Higuchi I, Nakagawa M, Saito M, Hirata K, Suehara M, Yoshida Y, Takahashi T, Aoki M, Osame M: Miyoshi myopathy patients with novel 5′ splicing donor site mutations showed different dysferlin immunostaining at the sarcolemma. Acta Neuropathol (Berl) 2002, 104:615–620
5. Weiler T, Bashir R, Anderson LV, Davison K, Moss JA, Britton S, Nylen E, Keers S, Vafiadaki E, Greenberg CR, Bushby CR, Wrogemann K:

Identical mutation in patients with limb girdle muscular dystrophy type 2B or Miyoshi myopathy suggests a role for modifier gene. Hum Mol Genet 1999, 8:871–877
6. Han R, Bansal D, Miyake K, Muniz VP, Weiss RM, McNeil PL, Campbell KP: Dysferlin-mediated membrane repair protects the heart from stress-induced left ventricular injury. J Clin Invest 2007, 117: 1805–1813
7. Anderson LV, Davison K, Moss JA, Young C, Cullen MJ, Walsh J, Johnson MA, Bashir R, Britton S, Keers S, Argov Z, Mahjneh I, Fougerousse F, Beckmann JS, Bushby KM: Dysferlin is a plasma membrane protein and is expressed early in human development. Hum Mol Genet 1999, 8:855–861
8. Achanzar WE, Ward S: A nematode gene required for sperm vesicle fusion. J Cell Sci 1997, 110 (Pt 9):1073–1081
9. Bashir R, Britton S, Strachan T, Keers S, Vafiadaki E, Lako M, Richard I, Marchand S, Bourg N, Argov Z, Sadeh M, Mahjneh I, Marconi G, Passos-Bueno MR, Moreira Ede S, Zatz M, Beckmann JS, Bushby K: A gene related to Caenorhabditis elegans spermatogenesis factor fer-1 is mutated in limb-girdle muscular dystrophy type 2B. Nat Genet 1998, 20:37–42
10. Rizo J, Sudhof TC: C2-domains, structure and function of a universal Ca2+-binding domain. J Biol Chem 1998, 273:15879–15882
11. Selcen D, Stilling G, Engel AG: The earliest pathologic alterations in dysferlinopathy. Neurology 2001, 56:1472–1481
12. Bansal D, Miyake K, Vogel SS, Groh S, Chen CC, Williamson R, McNeil PL, Campbell KP: Defective membrane repair in dysferlin-deficient muscular dystrophy. Nature 2003, 423:168–172
13. Confalonieri P, Oliva L, Andreetta F, Lorenzoni R, Dassi P, Mariani E, Morandi L, Mora M, Cornelio F, Mantegazza R: Muscle inflammation and MHC class I up-regulation in muscular dystrophy with lack of dysferlin: an immunopathological study. J Neuroimmunol 2003, 142:130–136
14. Gallardo E, Rojas-Garcia R, de Luna N, Pou A, Brown RH, Jr., Illa I: Inflammation in dysferlin myopathy: immunohistochemical characterization of 13 patients. Neurology 2001, 57:2136–2138
15. Nguyen K, Bassez G, Krahn M, Bernard R, Laforet P, Labelle V, Urtizberea JA, Figarella-Branger D, Romero N, Attarian S, Leturcq F, Pouget J, Levy N, Eymard B: Phenotypic study in 40 patients with dysferlin gene mutations: high frequency of atypical phenotypes. Arch Neurol 2007, 64:1176–1182
16. Ho M, Gallardo E, McKenna-Yasek D, De Luna N, Illa I, Brown RH Jr: A novel, blood-based diagnostic assay for limb girdle muscular dystrophy 2B and Miyoshi myopathy. Ann Neurol 2002, 51:129–133
17. De Luna N, Freixas A, Gallano P, Caselles L, Rojas-Garcia R, Paradas C, Nogales G, Dominguez-Perles R, Gonzalez-Quereda L, Vilchez JJ, Marquez C, Bautista J, Guerrero A, Salazar JA, Pou A, Illa I, Gallardo E: Dysferlin expression in monocytes: a source of mRNA for mutation analysis. Neuromuscul Disord 2007, 17:69–76
18. Nagaraju K, Rawat R, Veszelovszky E, Thapliyal R, Kesari A, Sparks S, Raben N, Plotz P, Hoffman EP: Dysferlin deficiency enhances monocyte phagocytosis: a model for the inflammatory onset of limb-girdle muscular dystrophy 2B. Am J Pathol 2008, 172:774–785
19. Kesari A, Pirra LN, Bremadesam L, McIntyre O, Gordon E, Dubrovsky AL, Viswanathan V, Hoffman EP: Integrated DNA, cDNA, and protein studies in Becker muscular dystrophy show high exception to the reading frame rule. Hum Mutat 2008, 29:728–737
20. Kaler SG, Devaney JM, Pettit EL, Kirshman R, Marino MA: Novel method for molecular detection of the two common hereditary hemochromatosis mutations. Genet Test 2000, 4:125–129
21. Brockington M, Yuva Y, Prandini P, Brown SC, Torelli S, Benson MA, Herrmann R, Anderson LV, Bashir R, Burgunder JM, Fallet S, Romero N, Fardeau M, Straub V, Storey G, Pollitt C, Richard I, Sewry CA, Bushby K, Voit T, Blake DJ, Muntoni F: Mutations in the fukutin-related protein gene (FKRP) identify limb girdle muscular dystrophy 2I as a milder allelic variant of congenital muscular dystrophy MDC1C. Hum Mol Genet 2001, 10:2851–2859
22. Expression profiling–best practices for data generation and interpretation in clinical trials. Nat Rev Genet 2004, 5:229–237
23. Li C, Wong WH: Model-based analysis of oligonucleotide arrays: expression index computation and outlier detection. Proc Natl Acad Sci USA 2001, 98:31–36
24. Seo J, Bakay M, Chen YW, Hilmer S, Shneiderman B, Hoffman EP: Interactively optimizing signal-to-noise ratios in expression profiling: project-specific algorithm selection and detection p-value weighting in Affymetrix microarrays. Bioinformatics 2004, 20:2534–2544
25. Seo J, Hoffman EP: Probe set algorithms: is there a rational best bet? BMC Bioinformatics 2006, 7:395
26. Jaiswal JK, Marlow G, Summerill G, Mahjneh I, Mueller S, Hill M, Miyake K, Haase H, Anderson LV, Richard I, Kiuru-Enari S, McNeil PL, Simon SM, Bashir R: Patients with a non-dysferlin Miyoshi myopathy have a novel membrane repair defect. Traffic 2007, 8:77–88
27. Kuroda TS, Fukuda M, Ariga H, Mikoshiba K: The Slp homology domain of synaptotagmin-like proteins 1–4 and Slac2 functions as a novel Rab27A binding domain. J Biol Chem 2002, 277:9212–9218
28. Lennon NJ, Kho A, Bacskai BJ, Perlmutter SL, Hyman BT, Brown RH Jr: Dysferlin interacts with annexins A1 and A2 and mediates sarcolemmal wound-healing. J Biol Chem 2003, 278:50466–50473
29. Ho M, Post CM, Donahue LR, Lidov HG, Bronson RT, Goolsby H, Watkins SC, Cox GA, Brown RH Jr: Disruption of muscle membrane and phenotype divergence in two novel mouse models of dysferlin deficiency. Hum Mol Genet 2004, 13:1999–2010
30. Campanaro S, Romualdi C, Fanin M, Celegato B, Pacchioni B, Trevisan S, Laveder P, De Pitta C, Pegoraro E, Hayashi YK, Valle G, Angelini C, Lanfranchi G: Gene expression profiling in dysferlinopathies using a dedicated muscle microarray. Hum Mol Genet 2002, 11:3283–3298
31. von der Hagen M, Laval SH, Cree LM, Haldane F, Pocock M, Wappler I, Peters H, Reitsamer HA, Hoger H, Wiedner M, Oberndorfer F, Anderson LV, Straub V, Bittner RE, Bushby KM: The differential gene expression profiles of proximal and distal muscle groups are altered in pre-pathological dysferlin-deficient mice. Neuromuscul Disord 2005, 15:863–877
32. Wenzel K, Zabojszcza J, Carl M, Taubert S, Lass A, Harris CL, Ho M, Schulz H, Hummel O, Hubner N, Osterziel KJ, Spuler S: Increased susceptibility to complement attack due to down-regulation of decay-accelerating factor/CD55 in dysferlin-deficient muscular dystrophy. J Immunol 2005, 175:6219–6225
33. Anderson LV, Harrison RM, Pogue R, Vafiadaki E, Pollitt C, Davison K, Moss JA, Keers S, Pyle A, Shaw PJ, Mahjneh I, Argov Z, Greenberg CR, Wrogemann K, Bertorini T, Goebel HH, Beckmann JS, Bashir R, Bushby KM: Secondary reduction in calpain 3 expression in patients with limb girdle muscular dystrophy type 2B and Miyoshi myopathy (primary dysferlinopathies). Neuromuscul Disord 2000, 10:553–559
34. Fukuda M: Versatile role of Rab27 in membrane trafficking: focus on the Rab27 effector families. J Biochem (Tokyo) 2005, 137:9–16
35. Kuroda TS, Fukuda M: Rab27A-binding protein Slp2-a is required for peripheral melanosome distribution and elongated cell shape in melanocytes. Nat Cell Biol 2004, 6:1195–1203
36. Fukuda M, Kuroda TS, Mikoshiba K: Slac2-a/melanophilin, the missing link between Rab27 and myosin Va: implications of a tripartite protein complex for melanosome transport. J Biol Chem 2002, 277:12432–12436
37. Wu XS, Rao K, Zhang H, Wang F, Sellers JR, Matesic LE, Copeland NG, Jenkins NA, Hammer JA, 3rd: Identification of an organelle receptor for myosin-Va. Nat Cell Biol 2002, 4:271–278
38. Nagaraju K, Raben N, Villalba ML, Danning C, Loeffler LA, Lee E, Tresser N, Abati A, Fetsch P, Plotz PH: Costimulatory markers in muscle of patients with idiopathic inflammatory myopathies and in cultured muscle cells. Clin Immunol 1999, 92:161–169
39. Park JJ, Berggren JR, Hulver MW, Houmard JA, Hoffman EP: GRB14. GPD1, and GDF8 as potential network collaborators in weight loss-induced improvements in insulin action in human skeletal muscle. Physiol Genomics 2006, 27:114–121
40. Bahadoran P, Aberdam E, Mantoux F, Busca R, Bille K, Yalman N, de Saint-Basile G, Casaroli-Marano R, Ortonne JP, Ballotti R: Rab27a: a key to melanosome transport in human melanocytes. J Cell Biol 2001, 152:843–850
41. Saegusa C, Tanaka T, Tani S, Itohara S, Mikoshiba K, Fukuda M: Decreased basal mucus secretion by Slp2-a-deficient gastric surface mucous cells. Genes Cells 2006, 11:623–631
42. Stinchcombe JC, Barral DC, Mules EH, Booth S, Hume AN, Machesky LM, Seabra MC, Griffiths GM: Rab27a is required for regulated secretion in cytotoxic T lymphocytes. J Cell Biol 2001, 152:825–834
43. Seabra MC, Mules EH, Hume AN: Rab GTPases, intracellular traffic and disease. Trends Mol Med 2002, 8:23–30
44. Menasche G, Pastural E, Feldmann J, Certain S, Ersoy F, Dupuis S, Wulffraat N, Bianchi D, Fischer A, Le Deist F, de Saint Basile G: Mutations in RAB27A cause Griscelli syndrome associated with haemophagocytic syndrome. Nat Genet 2000, 25:173–176